International Journal of Thermophysics, Vol. 5, No. 4, 1984

Contributions to the Heat Capacity of Solid Molybdenum in the Range 300–2890 K

A. Choudhury[1] **and C. R. Brooks**[1]

Received March 20, 1984

An analysis has been made of contributions to the heat capacity of Mo, with a special examination of the effect of the formation of vacancies near the melting point. Literature values of the heat capacity at constant pressure C_P were fitted to a polynomial. Using recent measurements of the velocity of sound at high temperature and literature data of the coefficient of expansion, the dilation correction was made to C_P to obtain the heat capacity at constant volume C_V. This heat capacity was taken to consist only of independent contributions from electron excitations (C_{VE}), harmonic lattice vibrations (C_{VH}), anharmonic lattice vibrations (C_{VA}), and the formation of vacancies (C_{VV}). Three models of C_{VE} (free electron, band theory, and electron-photon) have been used to calculate the electronic contribution, and an examination of the results indicates that the electron-phonon model is the best. C_{VH} is assumed to be given by the Debye model, with a single Debye temperature. Thus, the excess heat capacity $C_{VEX} = C_V - C_{VE} - C_{VH}$ is taken as equal to $(C_{VA} + C_{VV})$, where C_{VA} is linear with temperature ($C_{VA} = AT$), and we have fitted the values of C_{VEX} to determine the values of A and the energy and entropy of formation of vacancies which give the best fit. The anharmonic contribution is positive. The energy of vacancy formation is 100,000 J · mol^{-1}, in agreement with estimates by Kraftmakher from C_P data. The entropy of formation is 11.6 J · mol^{-1} · K^{-1}. The concentration of vacancies at the melting point (2890 K) is calculated to be 6.3%.

KEY WORDS: anharmonic heat capacity; compressibility; electronic heat capacity; lattice heat capacity; molybdenum; thermal expansion; vacancies.

1. INTRODUCTION

In pure molybdenum the heat capacity at constant pressure C_p shows a strong nonlinear increase as the melting point is approached. Although this

[1] Department of Chemical, Metallurgical and Polymer Engineering, The University of Tennessee, Knoxville, Tennessee 37996-2200, U.S.A.

0195-928X/84/1200-0403$03.50/0

increase may be caused by contributions from lattice vibrations and excitation of valence electrons, Kraftmakher [1–6] has championed the interpretation that this nonlinear increase is due solely to the formation of equilibrium lattice vacancies. He has analyzed the data to extract the energy and entropy of formation of monovacancies, and from these values has calculated that the equilibrium percentage of lattice sites vacant at the melting point is of the order of a few percent. However, criticism of his analysis exists [7–13], based mainly on observations of much lower vacancy concentrations at 300 K (room temperature) after quenching from near the melting point.

In the range 1300–1700 K, C_P is closely linear, and Kraftmakher has extrapolated this linear curve to higher temperatures to serve as a base heat capacity to subtract from C_P; this difference he then attributes to the formation of vacancies. The correct base heat capacity will be that associated with lattice vibrations (harmonic and anharmonic) and valence electron excitations, and is not necessarily linear above 1700 K. Thus, the energy and entropy of vacancy formation derived by Kraftmakher could be too high by the use of the linearly extrapolated base heat capacity.

In this paper, we have established more rigorously the base heat capacity, and then subtracted it from the experimental heat capacity to determine the contribution from the formation of vacancies. We have reviewed the literature for C_P, and fitted these data to a polynomial to represent C_P. Then we have converted C_P to the heat capacity at constant volume, C_V, by the dilation correction. We have then assumed that C_V can be represented by the sum of independent contributions from lattice vibrations (harmonic and anharmonic), excitation of valence electrons, and the formation of vacancies. We have used information in the literature to determine the former two contributions. From this approach, we have established a base heat capacity, which has allowed us to determine the energy and entropy of formation of vacancies in Mo, and the concentration at the melting point. The results have been compared with those obtained by Kraftmakher.

2. HEAT CAPACITY AT CONSTANT PRESSURE AND CONVERSION TO HEAT CAPACITY AT CONSTANT VOLUME

2.1. Heat Capacity at Constant Pressure, C_P

The temperature range over which the heat capacity is of interest is that between 300 and 2890 K. However, lower temperature data are of use in estimating the electronic contribution. Thus, the literature C_P data have been

assessed from 20 to 2890 K. For convenience of curve fitting, the data have been divided into two temperature ranges: 20–300 K and 300–2890 K.

For the lower temperature range, the data of Simon and Zeidler [14] and Clusius and Franzosini [15], which cover the range 20–300 K, have been accepted. These are shown in Fig. 1. For convenience 20 K has been taken as the lower limit for assessment. These data agree well with recent measurements of Khriplovich and Paukov [16]. (Hultgren et al. [17] have reviewed the other low temperature data, most of which are below 20 K.) The data were weighted equally and fitted by least squares to two polynomials, giving the curve shown in Fig. 1. All of the data are within ±1% of the curve. In the range 20–70 K,

$$C_P = -3.1298 + 0.0732T + 0.0012T^2 + 596.5968T^{-2}$$

and in the range 70–300 K, (1)

$$C_P = +7.8701 + 0.1118T - 0.0002T^2 - 35134.83T^{-2}$$

where C_P is in $J \cdot mol^{-1} \cdot K^{-1}$ and T in K.

In the range 300–2890 K, the sources of the 27 sets of data used are listed in Table I, along with brief comments about accuracy, temperature

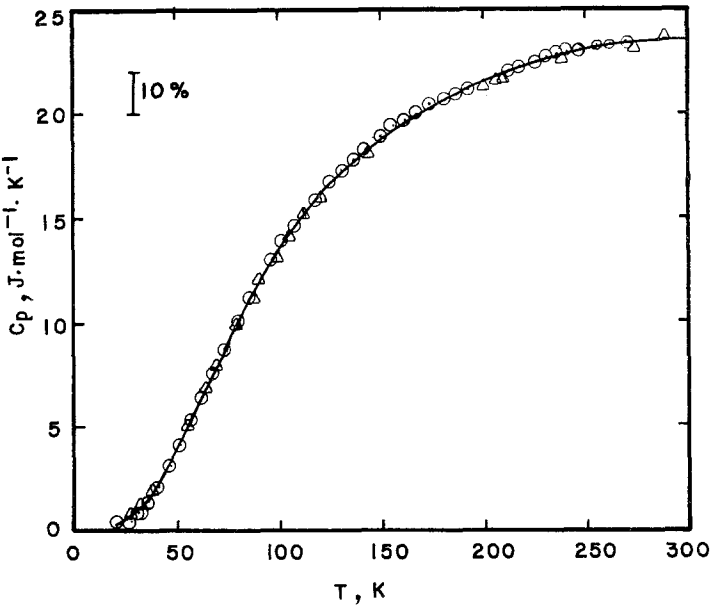

Fig. 1. C_P of Mo from 20 to 300 K. The solid line is the polynomial obtained by a least squares fit of the data. Circles, Clusius and Franzosini [15]; triangles, Simon and Zeidler [14].

Table I. Chronological Listing of C_P Data Sources

Ref. no.	Author(s)	Year	Temp. range (K)	Comments: Purity	Comments: Errors in C_P
14	Simon & Zeidler	1926	16–238		
18	Cooper & Langstroth	1928	233–523		2.4%
19	Stern	1928	273–717.5	99.97%	
20	Bronson et al.	1933	253.4–548.7		0.1% deviations
21	Jaeger & Veenstra	1934	273–1873		0.1–0.2%
22	Redfield & Hill	1951	481–1359		<4%
23	Horowitz & Daunt	1953	1.339–10.445	99.9%	
24	Lucks & Deem	1956	273–1923		
25	Fieldhouse et al.	1956	810–1810		3%
15	Clusius & Franzosini	1958	13.23–270.89	impurity = 0.0091%	
26	Rasor & McClelland	1959	1250–2750	impurity = 0.364%	±5%
27	Lazareva et al.	1960	1164–2540	impurity = 0.02%	1%
28	Lehman	1960	300–2800		
29	Kirillin et al.	1961	972.3–2610		enthalpy = ±0.4% temp. = 0.9–1.2%
30	Taylor & Finch	1961	200–2860		<4–7%
31	Lowenthal	1962	1288–2015	99.93%	0.5–1.5%
32	Rudkin et al.	1962	1550–2150	impurity 0.04–0.05%	<10%
33	Kirillin et al.	1963	273–2673		0.5–1.2%
3	Kraftmakher	1966	1300–2500		
34	Kirillin et al.	1968	972.5–2834.2		<5%
35	Makarenko et al.	1969	1100–2400	99.99%	10%
36	Dikhter & Lebedev	1970	2250–2850		<10%
37	Cezairliyan et al.	1970	1900–2800	impurity 0.04–0.06%	2–3%
38	Berezin et al.	1971	1900–2890		0.45–1.45%
39	Mebed et al.	1972	1300–2500		<4%
2	Kraftmakher	1973	1300–2500		
40	Chekhovskoi & Berezin	1973	298–2890	99.989–99.97%	2.35%
41	Fedorov	1975	500–2750		6–14%
42	Chekhovskoi & Kalinkina	1975	464–828	99.95%	1%
43	Lebedev et al.	1976	1500–2500		10%
44	Zhagrina et al.	1978	1–2892		

range, and purity (assumed to be mass %). All of the data from these sources were weighted equally and fitted by least squares to obtain the following polynomial: In the range 500–2890 K,

$$C_P = +25.0575 - 0.0013T + 0.3491 \times 10^{-5}T^2 \qquad (2)$$

where C_P is in $J \cdot mol^{-1} \cdot K^{-1}$ and T in K. Figure 2 shows all of the data points used and the curve corresponding to the polynomial. (Because of

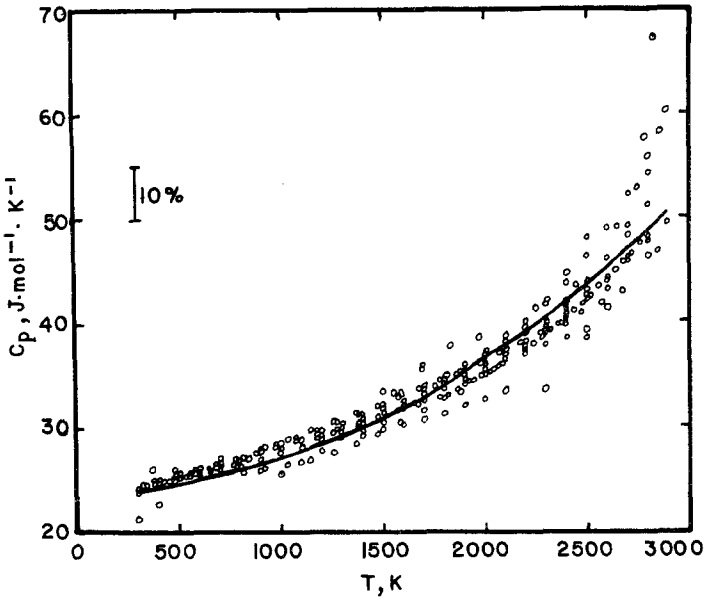

Fig. 2. C_P of Mo 300 to 2890 K showing the fit of the polynomial (the solid line) to all of the data.

disagreement between Eqs. (1) and (2) at 300 K, the value at 300 K in Table II was calculated from a polynomial fitted to the data from 150 to 2890 K.) With the exception of some very high temperature data of Dikhter and Lebedev [36], Jaeger and Veenstra [21], and Taylor and Finch [30], all the data are within ±10% of the curve. The polynomial agrees quite well with the National Bureau of Standards data [45] and around 2500 K is about 5% lower than those of Kraftmakher [3]. Values from all the polynomials are tabulated in Table II. In the following treatment, C_P of Mo was taken to be given by the polynomials.

2.2. Calculation of Dilation Correction and Conversion of C_P to C_V

C_V is calculated from C_P using the dilation correction

$$C_D = C_P - C_V = \alpha_V^2 VT/K_T \tag{3}$$

However, before the analysis can be made properly, C_V values should be converted to C_V at a fixed volume [46], usually taken at 0 K. This conversion [46] is given by

$$C_V - C_V(V_0) = (V - V_0)T\left[B_T\left(\frac{\partial \alpha_V}{\partial T}\right)_P + 2\alpha_V\left(\frac{\partial B_T}{\partial T}\right)_P + \alpha_V^2 B_T\left(\frac{\partial B_T}{\partial P}\right)_T\right] \tag{4}$$

Table II. The Quantities C_P, α_l, V, K_S, K_T, and C_V as a Function of Temperature for Mo

T (K)	C_P ($J \cdot mol^{-1} \cdot K^{-1}$)	α_l ($10^{-6} K^{-1}$)	V ($cm^3 \cdot mol^{-1}$)	K_S ($10^{-7} cm^2 \cdot N^{-1}$)	K_T ($10^{-7} cm^2 \cdot N^{-1}$)	C_V ($J \cdot mol^{-1} \cdot K^{-1}$)
2	0.0057					
4	0.0073					
6	0.0139					
8	0.0256					
10	0.0422					
15	0.1057					
20	0.3140	0.0650	9.3411	0.3777	0.3777	0.3140
40	2.1227	0.8059	9.3420	0.3781	0.3781	2.1221
60	5.8178	1.4882	9.3436	0.3786	0.3786	5.8149
80	10.0738	2.1118	9.3458	0.3790	0.3790	10.0659
100	13.5832	2.6767	9.3486	0.3794	0.3794	13.5673
150	18.6849	3.8324	9.3572	0.3803	0.3811	18.6361
200	21.5422	4.6214	9.3670	0.3812	0.3827	21.4477
250	23.0568	5.0439	9.3765	0.3820	0.3843	22.9163
300	23.9072	5.1221	9.4060	0.3847	0.3875	23.7371
500	25.2948	5.2653	9.4130	0.3906	0.3954	24.2703
700	25.8786	5.5010	9.444	0.3968	0.4038	25.0075
900	26.7416	5.8291	9.476	0.4032	0.4130	25.9340
1100	27.8839	6.2497	9.510	0.4100	0.4232	27.0150
1300	29.3056	6.7628	9.547	0.4171	0.4345	28.1299
1500	31.0065	7.3683	9.588	0.4245	0.4472	29.4349
1700	32.9868	8.0663	9.632	0.4322	0.4613	30.9079
1900	35.2463	8.8567	9.681	0.4402	0.4770	32.5242
2100	37.7852	9.7396	9.735	0.4485	0.4947	34.2570
2300	40.6034	10.7150	9.795	0.4571	0.5145	36.0784
2500	43.7008	11.7828	9.861	0.4660	0.5365	37.9596
2700	47.0776	12.9431	9.934	0.4753	0.5612	39.8714
2800	48.8707	13.5579	9.974	0.4800	0.5746	40.8294
2890	50.5443	14.1310	10.011	0.4843	0.5872	41.6895

where B_T is the isothermal bulk modulus ($1/K_T$) and P is the pressure. The first two terms can be estimated from data in the following sections, giving a value of $(4.8 \times 10^{-4} - 9.6 \times 10^{-4})$ N · cm^{-2} · K^{-2}. The last term in Eq. (4) cannot be calculated, as the pressure dependence of B_T is unknown. However, if we assume that this term is 9×10^{-4}, i.e., comparable to the first two terms and arbitrarily taken as positive, then at 2800 K, $C_V - C_V(V_0) \cong +0.3 J \cdot mol^{-1} \cdot K^{-1}$, which is a negligible correction. Thus in the following treatment, C_V has been taken to be an adequate approximation of $C_V(V_0)$.

2.2.1. *Coefficient of Expansion, α_V*

The coefficient α_V can be obtained from the linear coefficient of expansion α_l, since $\alpha_V = 3\alpha_l$. Values of α_l from 20 to 300 K are shown in Fig. 3(a), and in Fig. 3(b) for the range 300–2890 K. The sources of these data are shown in Table III. The data have been fitted to a polynomial for each range:

$$\text{20–300 K:} \quad \alpha_l = (-0.7346 + 0.0414T - 0.7332 \times 10^{-4}T^2) \times 10^{-6}$$

$$\text{300–2890 K:} \quad \alpha_l = (+5.0807 - 0.2086 \times 10^{-3}T + 0.1156 \times 10^{-5}T^2) \times 10^{-6} \tag{5}$$

where α_l is in K^{-1}. Values of α_l from these polynomials are tabulated in Table II. It is to be noted in Fig. 3 that in the low temperature range, the data are within ±5% of the curve, and within ±10% in the high temperature range, except for the four low points between 2000 and 2500 K and the two high points between 2500 and 2800 K.

2.2.2. *Molar Volume, V*

The molar volume V at 300 K was calculated from a density of 10.20×10^3 kg · m^{-3} [69] and an atomic mass of 95.94 [69]. From this value and the polynomial for α_V, the molar volume as a function of temperature was obtained using the following approach. The coefficient of volume thermal expansion is defined by

$$\alpha_V = 1/V(\partial V/\partial T)_P \tag{6}$$

Hence

$$\int_{V_0}^{V} dV/V = \int_{T_0}^{T} \alpha_V \, dT \tag{7}$$

where V_0 is the known molar volume at some temperature T_0, and V is the molar volume at a temperature T. Since α_l has been represented by polynomials of the form $A + BT + CT^2$, then α_V may be represented by $3(A + BT + CT^2)$, since $\alpha_V = 3\alpha_l$. Integrating Eq. (7):

$$\ln(V/V_0) = 3[A(T - T_0) + B(T^2 - T_0^2)/2 + C(T^3 - T_0^3)/3] \tag{8}$$

In this calculation $V_0 = 9.406$ cm^3 · mol^{-1} at $T_0 = 300$ K. Using Eq. (8), V was calculated over the temperature range of interest; the results are shown in Table II.

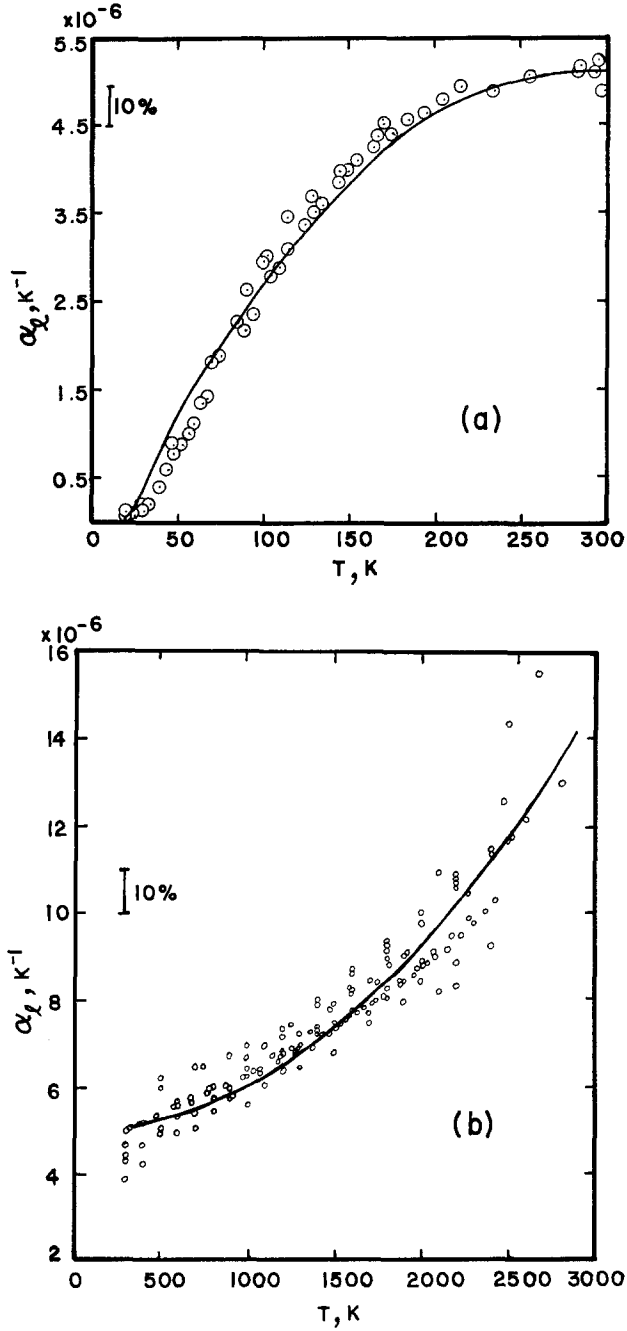

Fig. 3. The linear thermal expansion of Mo. The solid lines represent the polynomials fitted to the data: (a) in the range 20–300 K, and (b) in the range 300–2890 K.

Table III. Chronological Listing of α_l Data Sources

Ref. no.	Author(s)	Year	Comments
47	Worthing	1926	1000–2400 K Commercially very pure Mo
48	Nix & MacNair	1942	95–295 K 99.95 wt.% pure Mo
49	Demarquary	1945	400–2600 K
50	Edwards et al.	1951	1100–2500 K >99.9% pure Mo
51	Apblett & Pellini	1952	588–1922 K 99.9% pure Mo
25	Fieldhouse et al.	1956	300–1800 K Random error $\simeq$ 0.001 in.
26	Rasor & McClelland	1959	1300–2800 K 0.364% impurity, reproducibility 0.003 of specimen length
52	Totskii	1964	273–1373 K error = 1.2% at 373 K, 0.6% at 1273 K
53	Amonenko et al.	1964	523–2273 K error = <1–3%
54	Conway et al.	1965	300–2600 K 99.99% purity
55	Pawar	1967	301–795 K
56	Straumanis & Shodhan	1968	288–338 K 99.95% pure Mo, error ±0.05°C
57	Woodard	1969	30–170 K
58	Lebedev et al.	1969	10–285 K 99.9% pure Mo
59	Nasekovskii	1969	200–1200 K 99.999% pure Mo
60	Valentich	1969	500–2200 K 99.9% pure Mo
61	Chekhovskoi	1970	1173–2373 K 99.9–99.97% pure Mo, error = 1%
62	Straumanis & Woodard	1971	50–170 K
63	Petukhov & Chekhovskoi	1972	2023–2819 K 99.95% pure Mo
64	Lisovskii	1973	60–300 K 99.97% pure Mo
65	Waseda et al.	1975	300–2600 K 99.9% pure Mo, uncertainty = 2–3%
66	Amatuni et al.	1976	1073–2273 K 99.9–99.97% pure Mo
67	Petukhov et al.	1977	1274–2427 K error = ±0.9% at 1273 K, 0.6% at 2373 K
68	White et al.	1978	3 – 30 K and 65–100 K 99.9% pure Mo, max. discrep. = ±10%

2.2.3. *Isothermal Compressibility*, K_T

There are no data for K_T available over the temperature range of interest. However, velocity of sound measurements are available [70–73] so that the adiabatic compressibility K_S can be calculated. Figure 4 shows the calculated values. From these measurements we derive the K_S versus T curve in the range 20–2400 K. The data have been fitted to two polynomials by the least squares method. In the range 20–300 K,

$$K_s = (+0.3772 + 0.2306 \times 10^{-4}T - 0.1541 \times 10^{-7}T^2) \times 10^{-7} \qquad (9)$$

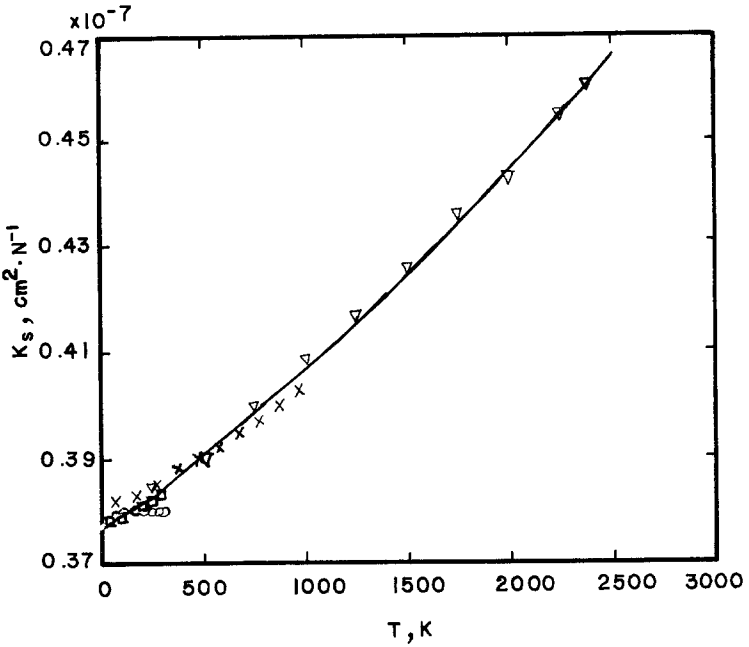

Fig. 4. Adiabatic compressibility K_S as a function of temperature for Mo. The solid line shows the polynomials from Eqs. (9) and (10) fitted to the data. ○, Featherson and Neighbours [72]; ▽, Bujard et al. [71]; □, Seidenkranz and Hegenbarth [73]; ×, Dickinson and Armstrong [70].

and in the range 300–2890 K,

$$K_s = (+0.3765 + 0.2622 \times 10^{-4}T + 0.3835 \times 10^{-8}T^2) \times 10^{-7} \quad (10)$$

where K_S is in $cm^2 \cdot N^{-1}$ and T in K. The latter polynomial, based on data only to 2400 K, was used for K_S to 2890 K. Values from the polynomials are listed in Table II. K_T is obtained from K_S [74] by the equation

$$K_T = K_S + \alpha_V^2 VT/C_P \quad (11)$$

K_T was calculated using values for the polynomials for K_S, α_V, V, and C_P. Values are listed in Table II.

2.2.4. Heat Capacity at Constant Volume, C_V

Using Eq. (3) and the values from the polynomials described in the preceding section, C_V has been calculated as a function of temperature; tabulated values are shown in Table II. Both C_P and C_V are plotted in Fig. 5.

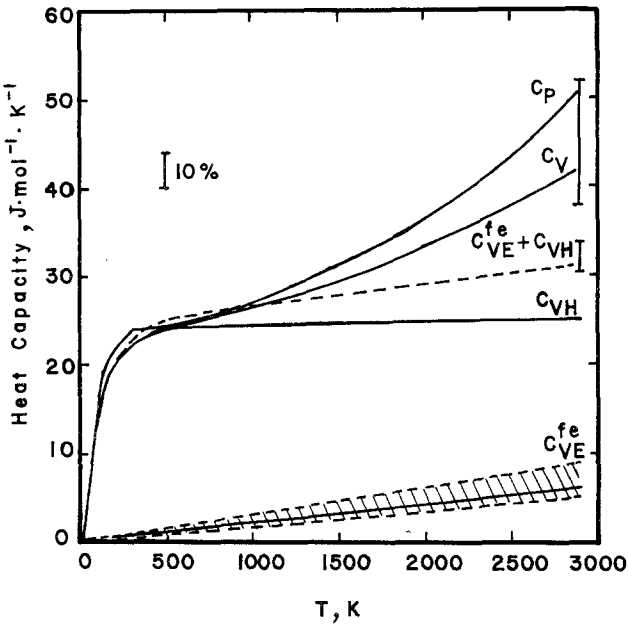

Fig. 5. C_P and C_V for Mo and some contributions to C_V.

The bar gives the estimated uncertainties in C_V, based on the estimated uncertainty for each quantity in Eq. (3).

3. PHYSICAL CONTRIBUTIONS TO C_V

The heat capacity C_V of molybdenum is taken to be the sum of independent contributions from harmonic lattice vibrations C_{VH}, anharmonic lattice vibrations C_{VA}, valence electron excitations C_{VE}, and the formation of lattice vacancies C_{VV}. Thus

$$C_V = C_{VH} + C_{VA} + C_{VE} + C_{VV} \tag{12}$$

3.1. Harmonic Lattice Vibration Contribution, C_{VH}

The contribution to C_V from harmonic lattice vibrations is taken from the Debye expression, using a single Debye temperature θ_D. θ_D can be obtained from low temperature C_P data, since, if the electronic heat capacity is given by γT, where γ is a constant, then:

$$C_V = C_{VH} + C_{VE} = 12\pi^4 R/5(T/\theta_D)^3 + \gamma T \tag{13}$$

where R is the gas constant. Thus a plot of C_V/T versus T^2 should be linear, and from the slope θ_D can be obtained. In Fig. 6 is shown such a plot using the data of Clusius and Franzosini [15] and Horowitz and Daunt [23]. The straight line is a least squares fit, and from it $\theta_D = 454$ K. Gscheidner [75] in his review of θ_D values gives a range of 388–474 K.

Using Beattie's [76] tables of $C_{VH}/3R$ versus (θ_D/T) and $\theta_D = 454$ K, values for C_{VH} were obtained, which are tabulated in Table IV, and the $C_{VH} - T$ curve is shown in Fig. 5. Above about 500 K, C_{VH} is quite insensitive to the value of θ_D. For example, at 900 K, a θ_D value of 388 K yields a C_{VH} of 24.7137 J · mol^{-1} · K^{-1}, while a θ_D value of 474 K yields a C_{VH} value of 24.5965 J · mol^{-1} · K^{-1}, which is a variation of approximately 0.5% in C_{VH} for a 86 K variation in θ_D.

Table IV. C_{VE} for Different Electronic Models and C_{VH} as a Function of Temperature for Mo[a]

T (K)	$C_{VE} = \gamma T$ (J·mol^{-1}·K^{-1})	C_{VE}^{b} (J·mol^{-1}·K^{-1})	C_{VE}^{ep} (J·mol^{-1}·K^{-1})	C_{VH} (J·mol^{-1}·K^{-1})
20				0.1667
40				1.3187
60				3.9690
80				7.3914
100				10.6460
150				16.4548
200				19.5434
250				21.2637
300	0.6548	0.75	0.05	22.3247
500	1.0913	1.37	0.15	23.9497
700	1.5278	2.10	0.30	24.4338
900	1.9644	2.80	0.45	24.6440
1100	2.4009	3.45	0.59	24.7446
1300	2.8374	4.10	0.70	24.8010
1500	3.2739	4.79	0.81	24.8412
1700	3.7105	5.43	0.92	24.8624
1900	4.1470	6.05	1.03	24.8814
2100	4.5835	6.70	1.13	24.8928
2300	5.0200	7.35	1.24	24.9033
2500	5.4566	8.00	1.35	24.9127
2700	5.8931	8.65	1.46	24.9171
2800	6.1130	8.95	1.51	24.9212
2890	6.3078	9.25	1.56	24.9212

[a] For C_{VE}, $\gamma = 21.83 \times 10^{-4}$; for C_{VE}^{ep}, $\gamma_0 = 5.4 \times 10^{-4}$.

3.2. Contribution From Valence Electron Excitations, C_{VE}

The electronic heat capacity is commonly given by

$$C_{VE} = 1/3\,\pi^2 K_B^2 N(E_F) T \tag{14}$$

where K_B is Boltzmann's constant, and $N(E_F)$ is the density of states at the Fermi surface. In the free electron model, $N(E_F)$ is temperature independent, and hence

$$C_{VE}^{fe} = \gamma T$$

as used in the preceding section, giving a value of $\gamma = 21.83 \times 10^{-4}$ J · mol^{-1} · K^{-2} as the intercept in Fig. 6. Hultgren et al. [17], in assessing the low temperature C_P data, chose a value of 18.1×10^{-4} from the data of Rorer et al. [77], noting that they used an extremely pure (99.999%) Mo sample. The recent measurements of Khriplovich and Paukov [16] gave 18.1×10^{-4}. Values of γ as high as 31.39×10^{-4} have been reported [78]. These upper and lower values give rise to the shaded portion in Fig. 5. The C_{VE}^{fe} obtained using the three values of γ quoted above is shown in Fig. 7.

Shimizu et al. [79, 80] have taken into account the shift in the density of states with temperature to obtain a temperature dependent electronic heat capacity coefficient $\gamma(T)$, so that $C_{VE}^{b} = \gamma(T)T$. The b here denotes band

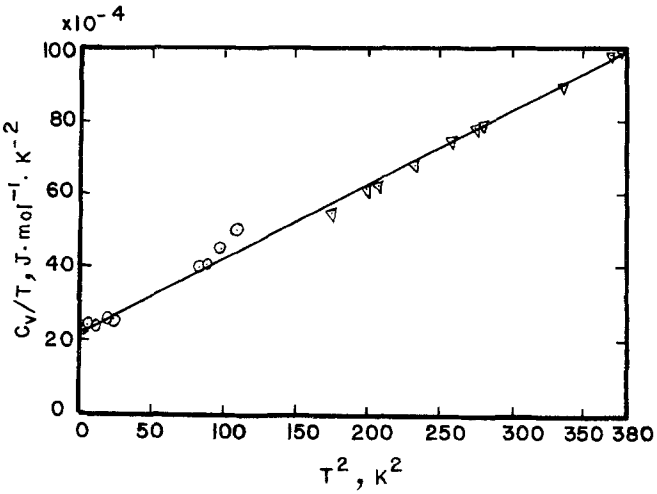

Fig. 6. C_V/T vs T^2 using low temperature (0–20 K) data. From the slope θ_D was calculated to be 454 K, and γ was calculated from the intercept to be 21.83×10^{-4} J · mol^{-1} · K^{-2}. ○, Horowitz and Daunt [23]; ▽, Clusius and Franzosini [15].

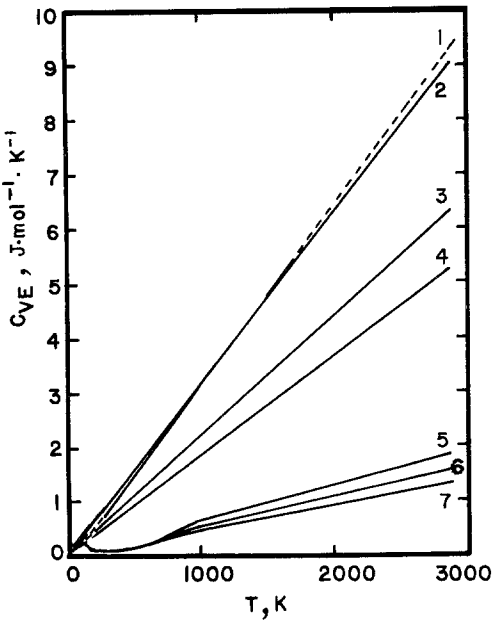

Fig. 7. Electronic heat capacity of Mo as a function of temperature using various electronic models. Free electron theory, C_{VE}^{fe}, band theory, C_{VE}^{b}, and electron-phonon interaction theory, C_{VE}^{ep}. Numbers on curves represent: 1, C_{VE}^{b};
2, C_{VE}^{fe} ($\gamma = 31.39 \times 10^{-4}$ J · mol^{-1} · K^{-2});
3, C_{VE}^{fe} ($\gamma = 21.83 \times 10^{-4}$ J · mol^{-1} · K^{-2});
4, C_{VE}^{fe} ($\gamma = 18.10 \times 10^{-4}$ J · mol^{-1} · K^{-2});
5, C_{VE}^{ep} ($\gamma_0 = 0.63 \times 10^{-3}$ J · mol^{-1} · K^{-2});
6, C_{VE}^{ep} ($\gamma_0 = 0.54 \times 10^{-3}$ J · mol^{-1} · K^{-2});
7, C_{VE}^{ep} ($\gamma_0 = 0.45 \times 10^{-3}$ J · mol^{-1} · K^{-2}).

theory. Shimizu's results are also shown in Fig. 7. Grimvall [81–83] has taken into account electron-phonon interactions, giving:

$$C_{VE}^{ep} = (\gamma_0 + \gamma_T)T = \gamma^{ep}T \tag{15}$$

where γ_0 is the coefficient in the absence of electron-phonon interactions and is calculated by Eq. (14) using the density of states at the Fermi level. Shimizu et al. [80] calculated $N(E_F) = 1 \times 10^{35}$ electron states/eV-mol, and Petroff and Viswanathan [84] obtained 0.73×10^{35}. These values give $\gamma_0 = 6.3 \times 10^{-4}$ and 4.5×10^{-4} J · mol^{-1} · K^{-2}, respectively. Using methods detailed in Grimvall's paper [82], C_{VE}^{ep} has been calculated for three values—the above two and for an average of these two of $\gamma_0 = 5.4 \times 10^{-4}$

$J \cdot mol^{-1} \cdot K^{-2}$. Table IV lists the results obtained using all three models, and they are shown graphically in Fig. 7. Since the three values of γ_0 used in Grimvall's approach yield such close results, the average value has been adopted for future calculations of C_{VE}^{ep}.

An insight into which model is most appropriate may be gained by noting that at temperatures $T > \theta_D$, C_{VH} given by the Debye model is rather insensitive to θ_D. At temperatures near θ_D, contributions from anharmonic lattice vibrations and from the formation of lattice vacancies should be negligible. Thus $C_{VH} + C_{VE}$ should show good agreement with C_V around 450 K; i.e., $C_V - C_{VH} - C_{VE} \cong 0$ near θ_D. The difference $C_V - C_{VH} - C_{VE}$ is shown in Fig. 8, where it is seen that the electron-phonon enhancement model gives the best agreement according to the previous statement.

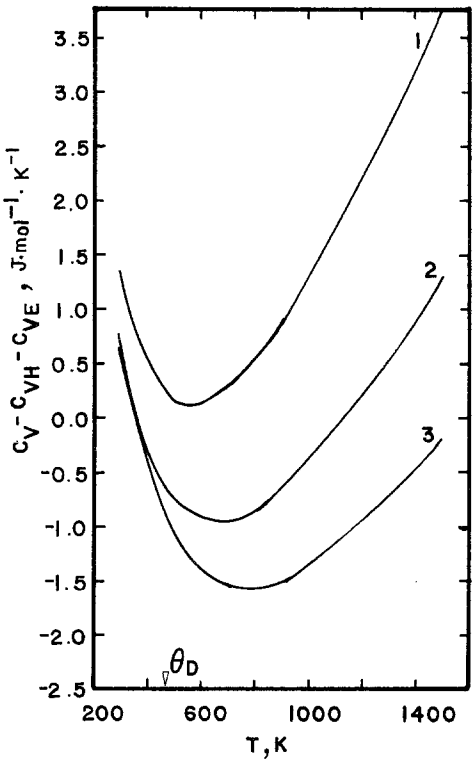

Fig. 8. $C_V - C_{VH} - C_{VE}$ as a function of temperature using various electronic models. Numbers on curves represent: 1, $C_V - C_{VH} - C_{VE}^{ep}$; 2, $C_V - C_{VH} - C_{VE}^{fe}$; 3, $C_V - C_{VH} - C_{VE}^{b}$.

3.3. Contributions From Anharmonic Lattice Vibrations, C_{VA}

The contribution of anharmonic lattice vibrations is rather difficult to determine since there is no theory sufficiently refined to allow its calculation from data independent of C_P. It is known that this contribution can be given approximately by AT, where A is a constant; but whether A is positive or negative cannot be determined from first principles [85]. From Eq. (12):

$$C_{VA} + C_{VV} = C_V - C_{VH} - C_{VE} \tag{16}$$

Since $C_{VA} + C_{VV}$ represents a left over quantity which has to be resolved into anharmonic and vacancy contributions, it is henceforth referred to as *excess specific heat* and is represented by $C_{VEX} = C_{VA} + C_{VV}$. The quantity $C_V - C_{VH} - C_{VE}$ is easily determined; the problem is in separating C_{VA} and C_{VV}. Various methods have been tried, and this section deals with these methods. Table V shows C_V, C_{VH}, C^{fe}_{VEX}, C^{b}_{VEX},C^{ep}_{VEX} as functions of temperature where C^{fe}_{VEX}, C^{ep}_{VEX}, and C^{b}_{VEX} are the C_{VEX}'s obtained using C_{VE} from the free electron theory, electron-phonon enhancement model, and the band theory, respectively.

If the temperature is not too high (e.g., below 1500 K), contributions from the formation of vacancies can be neglected. Also, if the temperature is above θ_D, then the harmonic lattice vibration contribution is given accurately by the Debye model. Taking $C_{VA} = AT$, then $AT = C_V - C_{VH} - C_{VE}$. C^{fe}_{VEX}, C^{ep}_{VEX}, C^{b}_{VEX} versus T can be plotted in the temperature range 300–1500 K, and the slope should yield A. Such a plot is shown in Fig. 8. It can be seen that all the models yield an approximately linear portion in the range 900–1300 K. Since the basic assumption in the approach is that the anharmonic contribution should disappear at and below θ_D, i.e., C^{fe}_{VEX}, C^{b}_{VEX}, $C^{ep}_{VEX} = 0$ near 450 K, it is seen that the electron-phonon enhancement model satisfies this assumption better than the other two models. Hence it would

Table V. The Quantities C_V, C_{VH}, C^{fe}_{VEX}, C^{ep}_{VEX}, and C^{b}_{VEX} as a Function of Temperature in the Range 300–1500 K

T (K)	C_V ($J \cdot mol^{-1} \cdot K^{-1}$)	C_{VH} ($J \cdot mol^{-1} \cdot K^{-1}$)	C^{fe}_{VEX} ($J \cdot mol^{-1} \cdot K^{-1}$)	C^{ep}_{VEX} ($J \cdot mol^{-1} \cdot K^{-1}$)	C^{b}_{VEX} ($J \cdot mol^{-1} \cdot K^{-1}$)
300	23.7371	22.3247	0.76	1.36	0.66
500	24.2703	23.9497	−0.77	0.17	−1.05
700	25.0075	24.4338	−0.95	0.27	−1.53
900	25.9340	24.6440	−0.67	0.84	−1.51
1100	27.0150	24.7446	−0.13	1.67	−1.18
1300	28.1299	24.8010	0.49	2.63	−0.77
1500	29.4349	24.8412	1.32	3.78	−0.20

seem from this and also section 3.2 that the electron-phonon enhancement model gives the best representation of the electronic contribution. From the slope of the linear portion of C_{VEX}^{ep} in Fig. 8, $A = 44.75 \times 10^{-4}\ \mathrm{J \cdot mol^{-1} \cdot K^{-2}}$.

Another approach which can be taken is that by Korshunov [86]. He noted that in the vicinity of $\theta_D \pm 0.3\theta_D$, the Thirring expansion can be used to yield

$$C_V(V_0) = 3R - \frac{R}{4}\left(\frac{h}{K_B}\right)^2 \langle \omega^2 \rangle \frac{1}{T^2} + C_{VE} + C_{VA} \tag{17}$$

where R is the gas constant, h is Planck's constant divided by 2π, K_B is Boltzmann's constant, and $\langle \omega^2 \rangle$ is the mean square of the phonon frequencies. In the region $< 1.3\theta_D$, C_{VA} may be assumed to be negligible so that $(C_V - C_{VE} - 3R)/T$ versus $1/T^3$ should be linear in this range and vanish at $1/T^3 = 0$. $C_V(V_0)$ is the heat capacity corrected to a constant volume V_0 at absolute zero. Here $C_V = C_V(V_0)$ as has been shown in the first part of section 2.2.

Figure 9 shows a plot of $(C_V - C_{VE} - 3R)/T$ versus $1/T^3$ in the range 300–1300 K for the three electronic models. It can be seen that all three

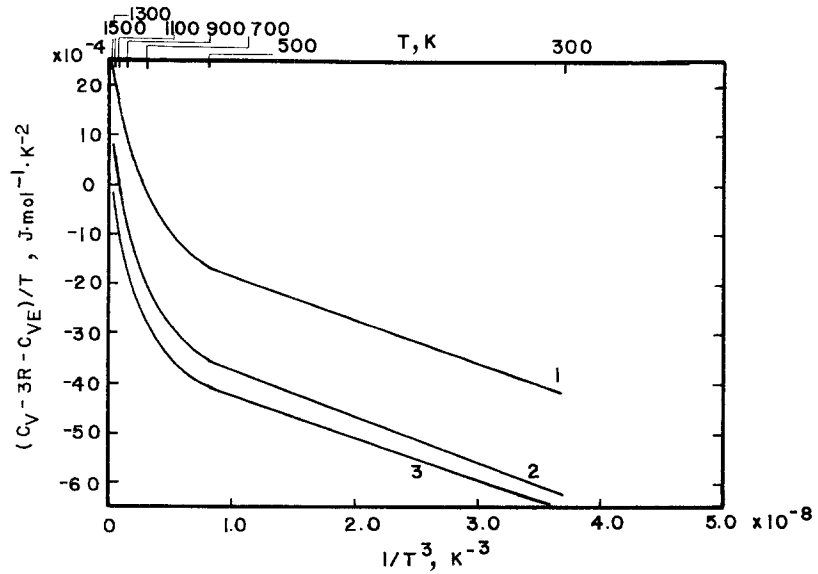

Fig. 9. $C_V - 3R - C_{VE}$ as a function of $1/T^3$ in the temperature range 300–1300 K for various electronic models. Numbers on curves represent: 1, $(C_V - 3R - C_{VE}^{ep})/T$; 2, $(C_V - 3R - C_{VE}^{fe})/T$; 3, $(C_V - 3R - C_{VE}^{b})/T$.

models yield a linear portion in the range 300–500 K and that the electron-phonon enhancement model does yield a straight line with the least intercept, though negative, thereby giving more credence to the conclusion drawn in section 3.2. However, the linearity is only approximate, for use of calculated values for C_V between 300 and 500 K will produce a slight curvature.

In his paper, Korshunov [86] gives a curve which is linear from 300 to 1300 K, with a positive intercept. Figure 10 shows Korshunov's plot where the intercept is the sum of A and an electronic heat capacity coefficient, from which he gets $A = 7 \times 10^{-4}\ \mathrm{J \cdot mol^{-1} \cdot K^{-2}}$. [Supposedly he converted C_V to $C_V(V_0)$, but it is not clear how he obtained the necessary data to find either C_V or $C_V(V_0)$]. In our treatment, the electron-phonon enhancement model yields $A = -9.5 \times 10^{-4}\ \mathrm{J \cdot mol^{-1} \cdot K^{-2}}$ (Fig. 9).

3.4. Contribution From Formation of Vacancies, C_{VV}

Assuming only monovacancies are involved, the contribution of vacancy formation to the heat capacity [1] is given by

$$C_{VV} = \frac{(\Delta E_f^V)^2}{RT^2} \exp(\Delta S_f^V/R) \exp(-\Delta E_f^V/RT) \tag{18}$$

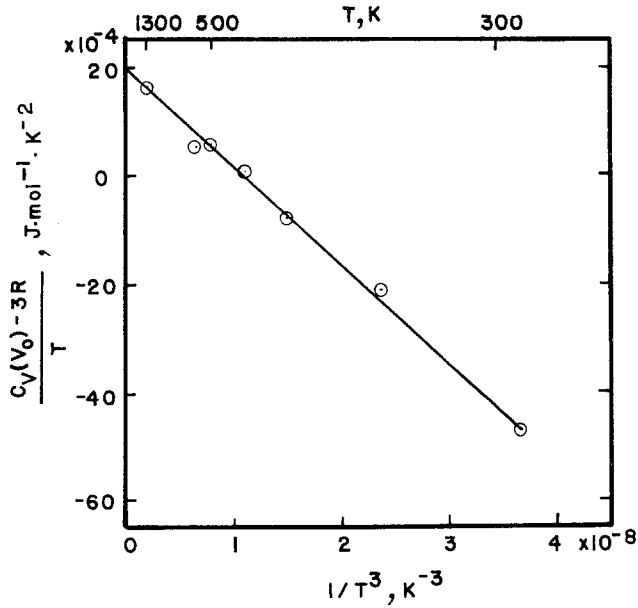

Fig. 10. Korshunov's [86] values for finding the anharmonic heat capacity of molybdenum.

where ΔE_f^V is the energy of vacancy formation, and ΔS_f^V is the entropy of vacancy formation. Thus $\ln(C_{VV}T^2)$ versus $1/T$ should yield a straight line whose slope $= -\Delta E_f^V/R$ and intercept $= \ln[(\Delta E_f^V)^2 \exp(\Delta S_f^V/R)/R]$. If the anharmonic contribution is negligible, $A = 0$. In section 3.3, A was found to be $+44.75 \times 10^{-4}$ or -9.5×10^{-4} J · mol^{-1} · K^{-2}. Since $C_{VV} = C_V - C_{VH} - C_{VA} - C_{VE}$, one can get a set of curves for each value of C_{VA}. Since vacancies are expected to form only at high temperatures, plots of $\ln(C_{VV}T^2)$ versus $1/T$ for the range 2100–2890 K are shown in Fig. 11 using all three electronic models. The values of ΔE_f^V, ΔS_f^V obtained are shown in Table VI.

Kraftmakher [1] has fitted his C_P versus T data between 1300 and 1700 K to a straight line and used the extrapolation of this to higher temperatures as a base heat capacity to subtract from C_P in order to obtain C_{VV}. The C_P and C_V data used in the present analysis in this temperature range are shown in Fig. 12. The $\ln(C_{VV}T^2)$ versus $1/T$ straight lines using Kraftmakher's method are shown in Fig. 11 (curve 5) and ΔE_f^V, ΔS_f^V and concentration of vacancies at the melting point calculated therefrom are tabulated in Table VI.

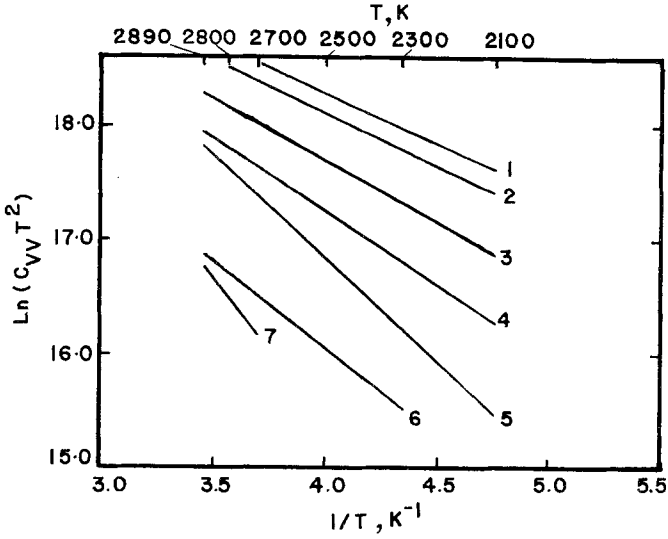

Fig. 11. The figure shows $\ln(C_{VV}T^2)$ as a function of $1/T$ in the temperature range 2100–2890 K using C_{VE} from various electronic models: free electron theory, *fe*; band theory, *b*; electron-phonon enhancement, *ep*. Numbers on curves represent: 1, *ep* ($A = -9.5 \times 10^{-4}$); 2, *ep* ($A = 0$); 3, *fe* ($A = 0$); 4, *b* ($A = 0$); 5, linear extrapolation of C_P; 6, linear extrapolation of C_V; 7, *ep* ($A = 44.75 \times 10^{-4}$).

Table VI. ΔE_f^V, ΔS_f^V, and Concentration of Vacancies at the Melting Point for Different Models

Model	ΔE_f^V (kJ·mol^{-1})	ΔS_f^V (J·mol^{-1}·K^{-1})	Vac. conc. at m.p. (%)
$C_{VV} = C_V - C_{VH} - C_{VE}^{fe}$ $(A = 0)$	90.83	11.15	8.73
$C_{VV} = C_V - C_{VH} - C_{VE}^{b}$ $(A = 0)$	106.76	11.31	4.58
$C_{VV} = C_V - C_{VH} - C_{VE}^{ep}$ $(A = 0)$	80.1	12.6	16.23
Linear extrapolation of C_p	151.6	20.03	2.03
Linear extrapolation of C_V	132.7	7.87	1.03
Kraftmakher [1]	215.5	48.6	4.3
$C_{VV} = C_V - C_{VH} - C_{VE}^{ep} - C_{VA}$ $(A = 44.75 \times 10^{-4})$	279.3	45.8	0.22
$C_{VV} = C_V - C_{VH} - C_{VE}^{ep} - C_{VA}$ $(A = -9.5 \times 10^{-4})$	76.84	13.53	20.8

Kraftmakher [4] has also indicated another approach to his model. Assuming that the anharmonic contribution may be represented by AT, the quantity $C_{VEX} = C_V - C_{VH} - C_{VE}$ may be represented by

$$C_{VEX} = AT + \frac{(\Delta E_f^V)^2}{RT^2} \exp\left(\frac{\Delta S_f^V}{R}\right) \exp\left(-\frac{\Delta E_f^V}{RT}\right) \tag{19}$$

Let

$$B = \Delta E_f^V, \quad C = \exp\left(\frac{\Delta S_f^V}{R}\right), \quad \text{and} \quad D = B^2 C/R$$

Then

$$C_{VEX} = AT + \frac{B^2 C}{RT^2} \exp\left(-\frac{B}{RT}\right) \tag{20}$$

and

$$\frac{C_{VEX}}{T} = A + \frac{D}{T^3} \exp(-B/RT) \tag{21}$$

If

$$X = [\exp(-B/RT)]/T^3 \quad \text{and} \quad Y = C_{VEX}/T$$

then

$$Y = A + DX \tag{22}$$

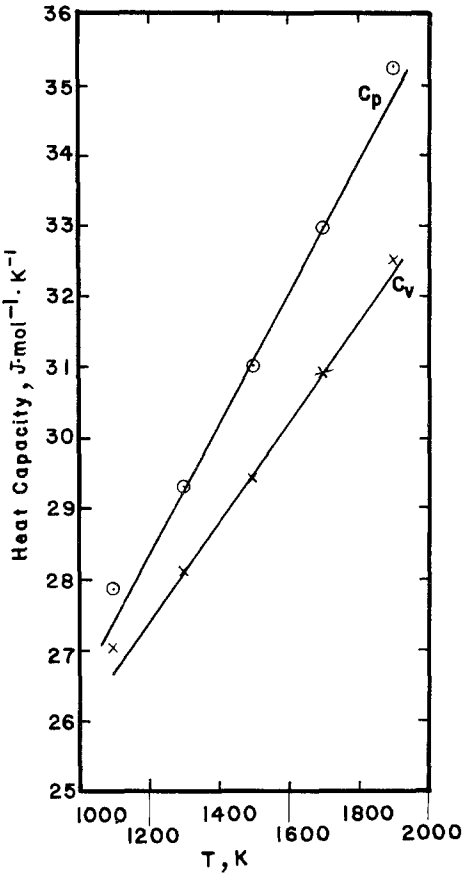

Fig. 12. C_p and C_V of Mo as a function of temperature in the range 1100–1900 K.

Hence Eq. (19) may be reduced to the straight line of Eq. (22). Assigning a range of reasonable values of ΔE_f^V (i.e., B), one may then calculate the standard deviation of Y from the best fit straight line of Y versus B. The value of ΔE_f^V corresponding to the minimum standard deviation would thus be the most probable ΔE_f^V value. Once this has been determined, one may calculate A and ΔS_f^V for this value of ΔE_f^V. The above procedure has been carried out for the three electronic models using values of C_V, C_{VH}, and C_{VE} in the temperature range 1500–2890 K. The results are shown graphically in Fig. 13, which shows that all three models yield a minimum at $\Delta E_f^V = 100{,}000\ \text{J} \cdot \text{mol}^{-1}$. Corresponding to this value, ΔS_f^V, A and the concentration of vacancies at the melting point are shown in Table VII.

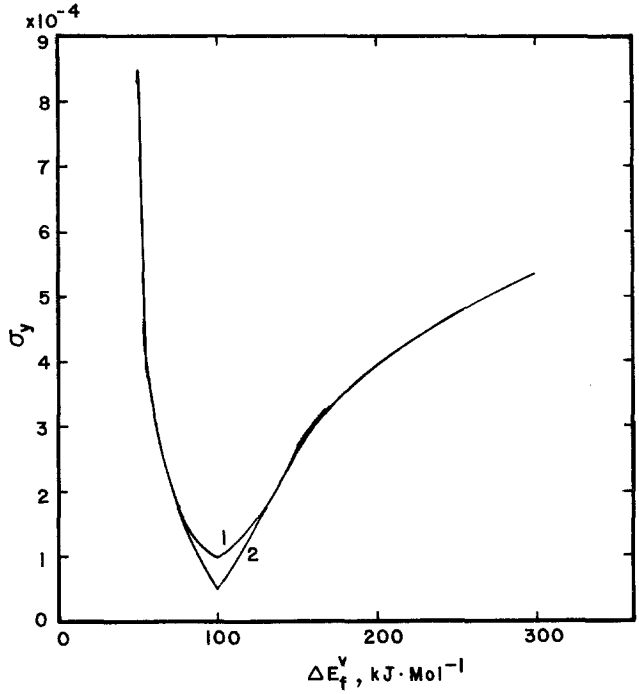

Fig. 13. Standard deviation of C_{VEX}/T as a function of ΔE_f^V. Numbers on curves represent: 1, free electron theory and band theory; 2, electron-phonon theory.

4. DISCUSSION

The relatively recent availability of high temperature velocity of sound data has allowed for the first time a rigorous calculation of C_V up to 2400 K. Above this temperature, C_V does suffer from uncertainty of the extrapolation of the K_S curve. However, it is clear that C_V increases nonlinearly above about 2100 K. Of the three assumed contributions to the heat capacity

Table VII. ΔE_f^V, ΔS_f^V, A, and Concentration of Vacancies for B Value Yielding Minimum σ_y for Different Electronic Models

	ΔE_f^V (kJ·mol^{-1})	ΔS_f^V (J·mol^{-1}·K^{-1})	A (J·mol^{-1}·K^{-1})	Conc. vac. at m.p. (%)
Free electron	100	11.6	1.0×10^{-2}	6.3
Electron-phonon	100	11.6	5.1×10^{-4}	6.3
Band theory	100	11.6	-4.9×10^{-4}	6.3

(lattice vibrations, electron excitations, and the formation of vacancies), models only exist for the calculation of the electronic contribution independent of the high temperature C_p data. Thus, upon subtracting from C_V the electron contribution, the remainder must be apportioned between lattice vibrations and the formation of vacancies.

The temperature dependence of the equilibrium vacancy contributions is given by Eq. (18), and for lattice vibrations, the Debye expression well represents the harmonic component. It is the anharmonic component that is not well defined theoretically; that is, lattice theories have not established the exact temperature dependence, and are not sufficiently refined to allow the calculation of the anharmonic contribution to C_V from information independent of C_p data. Considering these theoretical limitations, and the accuracy of the C_p data and thus of the derived C_V curve, the assumption of a linear anharmonic contribution is justified.

In our treatment, then, three electronic models have been used to obtain C_{VE}, which was subtracted from C_V. The simplest electronic model used was the free electron model, which has the electronic contribution varying linearly with temperature—the implicit assumption being that the constant of proportionality (electronic heat capacity coefficient) is temperature independent. In reality though, the electronic heat capcity coefficient is not temperature independent, and Shimizu [79] has developed a method based on band theory for calculating a temperature dependent heat capacity coefficient. Also, Grimvall [82] has shown a method for taking into account electron-phonon interaction, so that a temperature dependent electronic heat capacity coefficient can be calculated. Although these three models yield different C_{VE} curves, they are sufficiently similar so as not to significantly affect the subsequent analysis of contributions from anharmonic lattice vibrations and the formation of vacancies. Also, in spite of consideration being given to various estimates of the anharmonic term, it was found that the resulting energy and entropy of vacancy formation was not seriously affected by the value of the anharmonic contribution, except for the value $A = 44.75 \times 10^{-4}\ \mathrm{J \cdot mol^{-1} \cdot K^{-2}}$ (Table VI). This value yielded the highest energy of formation ($279.3\ \mathrm{KJ \cdot mol^{-1}}$) and the lowest concentration (0.2%) of vacancies at the melting point. However, using Kraftmakher's method to minimize the error in the difference between the sum of the contributions and the C_V values to obtain the best values of the energy and entropy of formation of vacancies and of A, values of ΔE_f^V and ΔS_f^V and of the concentration of vacancies at the melting point were essentially identical for the three values of A which were extracted (see Table VII). Since the electron-phonon electronic model seems to be the most appropriate, the anharmonic contribution would be positive (Table VII).

As far as the vacancy contribution is concerned, there seems to be two

Table VIII. Reported Values of ΔE_f^V and Concentration of Vacancies at the Melting Point

Ref. no.	Author(s) (Year)	ΔE_f^V ($kJ \cdot mol^{-1}$)	Vac. conc. at m.p. (%)	Method used
1	Kraftmakher (1964)	215.5	4.3	Specific heat measurement
	Present results	100	6.3	
92	Gorecki (1974)	216.0	≃10 at. %	Theory of melting
87	Meakin et al. (1965)	231.5	5×10^{-3}	Quenched in vacancies
88	Suezawa & Kimura (1973)	312.5	4.5×10^{-3}	Annealing of quenched in vacancies
89	Schwirlich & Schultz (1980)	308.6	1.1×10^{-3}	Resistivity studies on quenched specimens

distinct schools of thought. The major proponent of the first, Kraftmakher, predicts a relatively large equilibrium concentration of vacancies at the melting point (1–5%)—this is due to a relatively low energy of vacancy formation. *Per contra*, the other school feels that the concentration at the melting point should be exceedingly low; i.e., the energy of vacancy formation is relatively large. The conclusions of the latter school are based on the results of quenching experiments [7, 8, 11, 88–91] and on the simultaneous measurements of the lattice parameter and thermal expansion [93]. (An inherent problem with the quenching method is that one is never certain whether one has indeed succeeded in arresting all the vacancies existing at high temperatures. This concern assumes great importance since it affects the results and the analysis very drastically.) Table VIII compares then energy of formation of vacancies in Mo and their concentration at the melting point from analyses of heat capacity data to those from other types of experiments.

The primary conclusions from the present analysis are that Kraftmakher's analysis is essentially correct and that there is a real, positive contribution from the anharmonicity of lattice vibrations.

ACKNOWLEDGMENTS

This work was partially supported by the Department of Energy (contract DOE-DE-AS05-78ER-5951). We especially appreciate the careful examination of the paper by the reviewer.

REFERENCES

1. Ya. A. Kraftmakher, *Sov. Phys.-Sol. State* **6**(2):396 (1964).
2. Ya. A. Kraftmakher, *High Temp.-High Press.* **5**(4):433 (1973).
3. Ya. A. Kraftmakher, *Issled. Vys. Temp. Akad. Nauk. SSSR-Sib. Otd.*, 5 (1966).
4. Ya. A. Kraftmakher, *Scripta Met.* **11**:1033 (1977).
5. Ya. A. Kraftmakher, in *Int. Symp.-Defect Interactions in Solids* (I.I.S., Bangalore, India, 1972), p. 64.
6. Ya. A. Kraftmakher and P. G. Strelkov, in *Proc. Int. Conf. Vacancies and Interstitials in Metals* (North-Holland, Amsterdam, 1969), pp. 59–79.
7. M. Hoch, in ref. 6, pp. 81–90.
8. H. Schultz, *Mat. Sci. Eng.* **3**:189 (1968–69).
9. M. Hoch, in *Thermodyn. Nucl. Mat. Proc. Symp. 4th* (IAEA, Vienna, Austria, 1975), Vol. 2, pp. 113–122.
10. M. Hoch, in *Proc. Symp. Thermophys. Prop. 5* (ASME, New York, 1970), pp. 380–384.
11. K. Maier, M. Peo, B. Saile, H. E. Schaefer, and A. Seeger, *Phil. Mag. A* **40**(5):701 (1979).
12. A. Seeger, *Cryst. Lattice Defects* **4**(4):221 (1973).
13. R. W. Siegel, *J. Nucl. Mat.* **69–70**: 117 (1978).
14. F. Simon and W. Zeidler, *Z. Phys. Chem.* **123**:383 (1926).
15. K. Clusius and P. Franzosini, *Z. Naturforsch.* **14a**:99 (1959).
16. L. M. Khriplovich and I. E. Paukov, *J. Chem. Thermodyn.* **15**:333 (1983).
17. R. Hultgren, P. D. Desai, D. T. Hawkins, M. Gleiser, K. K. Kelley, and D. D. Wagman, *Selected Values of the Thermodynamic Properties of the Elements* (ASM, Metals Park, Ohio, 1973).
18. D. Cooper and G. Langstroth, *Phys. Rev.* **33**:243 (1929).
19. T. Stern, *Phys. Rev.* **32**:298 (1928).
20. H. L. Bronson, H. M. Chisholm, and S. M. Dockerty, *Can. J. Res.* **8**:282 (1933).
21. F. M. Jaeger and W. A. Veenstra, *Rev. Trav. Chim.* **53**:677 (1934).
22. T. A. Redfield and J. H. Hill, USAEC-ORNL (Oak Ridge National Laboratory, Oak Ridge, Tennessee, 1951).
23. M. Horowitz and J. G. Daunt, *Phys. Rev.* **31**:1099 (1953).
24. C. F. Lucks and H. W. Deem, WADC Tech. Rept. 55-496, Battelle Memorial Inst., Columbus, Ohio (1956), p. 43.
25. I. B. Fieldhouse, J. C. Hedge, J. I. Lang, A. N. Takata, and T. E. Waterman, WADC Tech. Rept. 55-495 Part I, Wright Air Dev. Center, Wright-Patterson Air Force Base, Ohio (1956).
26. N. S. Rasor and J. D. McClelland, *Phys. Chem. Solids* **15**:17 (1960).
27. L. S. Lazareva, P. B. Kantor, and V. V. Kandyba, *Phys. Met. Metallog.* **11**:133 (1961).
28. G. W. Lehman, WADD Tech. Rept. 60-581, Atomics Int., Canoga Park, Calif. (1960).
29. V. A. Kirillin, A. E. Sheindlin, and V. Ya. Chekhovskoy, *Dokl. Akad. Nauk. SSSR* **139**(3):645 (1961).
30. R. E. Taylor and R. A. Finch, Atomics Int. N.A.A., SR-6034, Canoga Park, Calif. (1961).
31. G. C. Lowenthal, *Aust. J. Phys.* **16**:47 (1963).
32. R. L. Rudkin, W. J. Parker, and R. J. Jenkins, *Temp. Meas. Cont. Sci. Ind.* **3**:523 (1962).
33. V. A. Kirillin, A. E. Sheindlin, and V. Ya. Chekhovskoy, *High Temperature Technology*, IUPAC-Proc. Int. Symp. High Temp. Tech. (Butterworths, London, 1964), pp. 471–484.
34. V. A. Kirillin, A. E. Sheindlin, V. Ya. Chekhovskoi, and V. A. Petrov, *Teplofiz. Svoistva. Veshchestv.* (Leningrad Teckhnol. Inst. Kholod. Prom., Leningrad, U.S.S.R., 1969), Vol. 3, pp. 80–87.

35. I. N. Makarenko, L. N. Trukhanova, and L. P. Fillipov, *High Temp.* **8**(2): 416 (1970).
36. I. Ya. Dikhter and S. V. Lebedev, *High Temp.* **9**(5):845 (1971).
37. A. Cezairliyan, M. S. Morse, H. A. Berman, and C. W. Beckett, *J. Res. Natl. Bur. Stand.* **74(a)**:65 (1970).
38. B. Ya. Berezin, V. Ya. Chekhovskoi, and A. E. Sheindlin, *High Temp.-High Press.* **3**:287 (1971).
39. M. M. Mebed, R. P. Yurchak, and L. P. Filippov, *High Temp.-High Press* **5**(3):253 (1973).
40. V. Ya. Chekhovskoi and B. Ya. Berezin, *Teplofiz. Svoistva. Tverd. Veshchestv. Mater. Konf. 4* (Nauka, Moscow, U.S.S.R., 1973), pp. 128–134.
41. V. B. Fedorov, *High Temp.* **13**(3):608 (1975).
42. V. Ya. Chekhovskoi and R. G. Kalinkina, *Zh. Fiz. Khim.* **49**(3):740 (1975).
43. S. V. Lebedev, A. I. Savvatimskii, and M. A. Sheindlin, *High Temp.* **14**(2):259 (1976).
44. G. A. Zhagrina, L. R. Fokin, and V. Ya. Chekhovskoi, Teplofiz. Svoistva. Veschestv. Pri. Vysok. Temp., 1978 (Ref. Zh. Fiz. E., Abstr. No. 1E327, 1979).
45. D. A. Ditmars, A. Cezairliyan, S. Ishihara, and T. B. Douglas, Enthalpy and Heat Capacity Standard Reference Material: Molybdenum SRM781, From 273 to 2800 K, N.B.S. Spec. Publ. 260-55-1977.
46. V. A. Korshunov, *Phys. Met. Metallog.* **41**(2):54 (1976).
47. A. G. Worthing, *Phys. Rev.* **28**(1):190 (1926).
48. F. C. Nix and D. MacNair, *Phys. Rev.* **61**:74 (1942).
49. J. Demarquay, *Compt. Rend.* **220**(2):81 (1945).
50. J. W. Edwards, R. Speiser, and H. L. Johnston, *J. Appl. Phys.* **22**(4):424 (1951).
51. W. R. Apblett and W. S. Pellini, *Trans. Am. Soc. Met.* **44**(6):1200 (1952).
52. E. E. Totskii, *High Temp.* **2**(2):181 (1964).
53. V. M. Amonenko, P. N. V'yugov, and V. S. Gumenyuk, *High Temp.* **2**(1):22 (1964).
54. J. B. Conway, R. A. Hein, R. M. Fincel, and A. C. Losekamp, Enthalpy and Thermal Expansion of Several Refractory Metals to 2500°C, USAEC. Publ-GE-TM-64-2-8 (General Electric Co., Cincinnati, Ohio, Advanced Technology Services, Feb. 1964).
55. R. Pawar, *Curr. Sci.* **36**(16):428 (1967).
56. M. E. Straumanis and R. P. Shodhan, *Trans. Met. Soc. (AIME)* **242**:1185 (1968).
57. C. L. Woodard, X-ray determination of lattice parameters and thermal expansion coefficients of aluminum, silver and molybdenum at cryogenic temperatures, Diss. Abstr. Int. B 1970, **31**(1):225 (1969).
58. V. P. Lebedev, A. A. Mamlui, V. A. Pervakov, N. S. Petrenko, V. P. Popov, and V. I. Khotkevich, *Ukr. Fiz. Zh.* **14**(5):746 (1969).
59. A. P. Nasekovskii, *Izv. Vys. Ucheb. Zaved. Fiz.* **12**(1):65 (1969).
60. J. Valentich, *Instrum. Contr. Syst.* **42**(10):91 (1969).
61. V. Ya. Chekhovskoi and V. A. Petukhov, in *Proc. 5th Symp. Thermophys. Prop.* (ASME, New York, 1970), pp. 366–372.
62. M. E. Straumanis and C. L. Woodard, *Acta. Cryst.* **A27**(6):549 (1971).
63. V. A. Petukhov and V. Ya. Chekhovskoi, *High Temp.-High Press.* **4**(6):671 (1972).
64. Yu. A. Lisovskii, *Sov. Phys.-Sol. State* **14**:2015 (1973).
65. Y. Waseda, K. Hirata, and M. Ohtani, *High Temp.-High Press.* **7**(2):221 (1975).
66. A. N. Amatuni, T. I. Malyutina, V. Ya. Chekhovskoi, and V. A. Petukhov, *High Temp.-High Press.* **8**(5):565 (1976).
67. V. A. Petukhov, V. Ya. Chekhovskoi, and A. G. Mozgovoi, *High Temp.* **15**(1):175 (1977).
68. G. K. White, T. F. Smith, and R. H. Carr, *Cryogenics* **18**(5):301 (1978).
69. *Handbook of Chemistry and Physics*, R. C. Weast, ed., 55th ed. (CRC, 1974–75).

70. J. M. Dickinson and P. E. Armstrong, *J. Appl. Phys.* **38**(2):602 (1967).
71. P. Bujard, R. Sanjines, E. Walker, J. Ashkenazi, and M. Peter, *J. Phys. F.* **11**:775 (1981).
72. F. H. Featherson and J. R. Neighbours, *Phys. Rev.* **130**:1327 (1963).
73. V. T. Seidenkranz and E. Hegenbarth, *Exp. Technik Physik* (Berlin) **26**(1):13 (1978).
74. M. W. Zemansky, *Heat and Thermodynamics*, 3rd ed. (McGraw-Hill, New York, 1951).
75. K. A. Gscheidner, *Sol. State Phys.* **16**:275 (1964).
76. J. A. Beattie, *J. Math. Phys.* (MIT) **6**:1 (1926).
77. D. C. Rorer, D. G. Orr, and H. Meyer, *Phys. Rev.* **138**:1661 (1965).
78. N. M. Wolcott, Conf. Phys. Des Bass. Temp., Bulletin de l'Institut International du Froid, Annexe, 286 (1955).
79. M. Shimizu, Natl. Bur. Stands. (U.S.) Spec. Pub. 323 (1971), pp. 685–691.
80. M. Shimizu, A. Katsuki, and K. Ohmori, *J. Phys. Soc. Japan* **21**(10):1922 (1966).
81. G. Grimvall, *Phys. Kondens. Mat.* **11**:279 (1970).
82. G. Grimvall, *J. Phys. Chem. Solids* **29**:1221 (1965).
83. G. Grimvall, *Phys. Scripta* **14**:63 (1976).
84. I. Petroff and C. R. Vishwanathan, *Natl. Bur. Stands. (U.S.) Spec. Publ. 323* (1971), pp. 53–56.
85. R. C. Shukla, *Int. J. Thermophys.* **1**(1):73 (1980).
86. V. A. Korshunov, *Phys. Met. Metallog.* **48**(1):53 (1979).
87. J. D. Meakin, A. Lawley, and R. C. Koo, *Lattice Defects in Quenched Metals-Proc. Int. Conf.* (Academic Press, New York, 1965), pp. 767–769.
88. M. Suezawa and H. Kimura, *Phil. Mag.* **28**(4):901 (1973).
89. I. A. Schwirlich and H. Schultz, *Phil. Mag. A* **42**(5):601 (1980).
90. A. Seeger and H. Mehrer, in ref. 6, pp. 1–58.
91. J. Nihoul, in ref. 6, pp. 839–888.
92. T. Gorecki, *Z. Metallk.* **65**(4):426 (1974).
93. R. O. Simmons and R. W. Balluffi, *Phys. Rev.* **129**(4):1533 (1963).